

Polarization Effects for Indoor Wireless Communications at 60 GHz

Ferhat Yıldırım, *Student Member, IEEE*, Ali S. Sadri, and Huaping Liu, *Member, IEEE*

Abstract—This letter studies the performance of indoor wireless communication systems operating at 60 GHz with different polarization schemes. Circular polarization is known to reduce multipath effects in line-of-sight (LOS) environments in the 60 GHz band. We propose a modified channel model based on the IEEE 802.15.3c channel model to incorporate the polarization effects. We then use this model to evaluate the error performance of a wireless communication system that uses circular polarization. The results are compared with linear polarization for LOS environments.

Index Terms—Circular polarization, 60 GHz communications, channel models.

I. INTRODUCTION

THE 60 GHz unlicensed spectrum (57–64 GHz) is attractive for high-speed wireless personal area networks in indoor environments. It is well known that multipath effects cause intersymbol interference (ISI) for high-speed signaling and ultimately limit the achievable data rate at any frequency band. The spatial and temporal properties of the 60 GHz channel are quite different than those of the lower frequency bands [1], [2]; this leads to the need of novel approaches to mitigate multipath effects in the 60 GHz band. Several approaches have been proposed to improve the performance of the 60 GHz wireless systems through phase noise suppression and different modulation techniques [2]–[4]. Use of directional antennas is also an effective method to mitigate multipath effects for the 60 GHz band [5]–[7].

In this letter, we study the possibility of using different polarizations to alleviate the multipath effect at 60 GHz. We modify the IEEE 802.15.3c channel model to incorporate the effect of circular polarization and numerically evaluate the improvement of using circular polarization in line-of-sight (LOS) propagation environments.

II. CHANNEL MODEL WITH CIRCULAR POLARIZATION

A. Circular polarization

In LOS communication environments, reflected, diffracted, and scattered waves from the nearby objects (i.e., indirect paths) cause multipath fading effects. It has been found based on the measurements in [8] that reflection is the dominating factor affecting the channel delay at 60 GHz, whereas the significance of diffraction and penetration decreases as frequency increases. Hence, at 60 GHz, one can control the channel delay by changing the reflection characteristics of the wave, which depends on the reflecting material and the

incident wave (polarization and the incident angle) [9]. Since channel delay relative to the bit interval determines the level of ISI, the reflection characteristic of waves has a direct influence on the error performance of the wireless communication systems at 60 GHz. The simplest way to change the reflection characteristics of a wave is to change its polarization.

The reflection characteristic of circularly polarized waves is quite different from that of linearly polarized waves. For certain incident angles the handedness of a circularly polarized wave switches upon reflection [10]. Theoretically, a circularly polarized antenna rejects a cross polarized incoming wave; however, in practice, the received wave would experience a finite attenuation (e.g., 20 dB). Even with this finite attenuation, appropriate use of polarization could lead to significantly reduced channel delay spread, and hence improved error performance for high-rate communications.

B. Impulse response model

Several channel models (e.g., [11]–[14]) and measurement results (e.g., [15], [16]) can be found in the literature along with our more recent measurement results [17] for the 60 GHz band. In this letter, we use a similar channel model that is developed by the IEEE 802.15.3c Task Group [12], which models both time and angle of arrival statistics of the received rays. We use a time-dependent variation of this model to compare the effects of polarization on the system performance. The channel impulse response of this model is expressed as

$$h(t) = a_{\text{LOS}}\delta(0) + \sum_{l=0}^{L-1} \sum_{k=0}^{K-1} a_{l,k}\delta(t - T_l - \tau_{l,k}) \quad (1)$$

where T_l and $\tau_{l,k}$ are the arrival times for clusters and rays within a cluster, respectively, a_{LOS} is the coefficient for the direct path, and $a_{l,k}$ is the coefficient of the k -th ray of the l -th cluster.

Several scenarios have been proposed in [12]. In this letter, we focus on indoor LOS models CM1, CM5, and CM10 for residential room, library, and hallway scenarios, respectively. For practical systems that operate at high data rates in the 60 GHz band, the deployment is most likely required to have an LOS component between the transmitter and the receiver. Thus, these environments represent a useful scenario that is likely to be encountered in practice. We assume that both the transmitter and receiver are equipped with an omnidirectional antenna.

Although deployment of most of the 60 GHz networks is for LOS environments, NLOS scenarios cannot be avoided. In NLOS environments, due to the high penetration loss of 60 GHz signals through objects, reflected paths must be relied on for effective communications. In such a case, directive antennas could increase the system performance by focusing the radiated power in a certain direction. However, networks with directional antennas require more sophisticated medium access

Manuscript received May 15, 2008. The associate editor coordinating the review of this letter and approving it for publication was G. Mazzini.

F. Yıldırım and H. Liu are with the School of Electrical Engineering and Computer Science, Oregon State University, Corvallis, OR 97331 USA (e-mail: {yildiria, hliu}@eecs.oregonstate.edu).

A. S. Sadri is with WPAN/mmWave Technology, Intel Corporation, Santa Clara, CA, USA (e-mail: ali.s.sadri@intel.com).

Digital Object Identifier 10.1109/LCOMM.2008.080757.

control (MAC) algorithms. Issues with 60 GHz networks using directional antennas along with a proposed directional MAC algorithm are discussed in [18].

C. Incorporation of polarization

The model proposed by the IEEE 802.15.3c Task Group [12] is based on linear polarization. Thus, we need to modify the model given in (1) to incorporate the effects of circular polarization.

In multipath environments, each path may experience multiple reflections before it reaches the receiver. Let m represent the order-of-arrival (OoA) of paths. The incident angle of each reflection, θ_i , is an independent and identically distributed random variable. We define a threshold angle, θ_T , for which the handedness of the circular polarization switches after reflection when $\theta_i \leq \theta_T$. The value of θ_T depends on the material properties of the reflective surface. The probability of handedness being switched after a reflection can be written as $p_s = F_{\theta_i}(\theta_T)$, where $F(\cdot)$ is the cumulative distribution function of θ_i .

Let p_a represent the probability that a path experiences odd number of handedness switching from the transmitter to the receiver. Such a path will be significantly attenuated (or eliminated in the ideal case) due to cross-pol suppression. In order to incorporate the effect of circular polarization into the channel model (1), we need to establish the relationship between p_a , which depends on p_s , and m . Note that for the LOS path ($m = 0$), $p_a = 0$.

For simplicity, let us consider the first 50 multipath components. This is sufficient for most practical applications since paths arrived after this large index would be too weak to have a non-negligible impact on the system performance. From extensive ray tracing simulation results, we observe that the statistical behavior of early-arrival paths ($m \leq 11$) is different than that of later-arrival ones ($m > 11$). For all channel model scenarios considered (library, hallway, and residential room), it is observed that the paths with $m \leq 11$ (excluding the LOS component) arrive at the receiver via either one or two reflections with a probability equal to 1. Therefore, for the OoA index region $m = (0, 11]$, the probability that a path will experience a significant cross-pol attenuation is expressed as

$$p_a = \lambda(m)p_s + 2(1 - \lambda(m))p_s(1 - p_s) \quad (2)$$

where $\lambda(m)$ is the probability of a path having only one reflection. Ray tracing simulations also show that the first two multipaths from the transmitter to the receiver have only one reflection with a probability 1 for all channel model scenarios. Hence, for $m = 1$ and 2, $\lambda(m) = 1$ and $p_a = p_s$.

The function $\lambda(m)$ is derived using the ray tracing simulation for all channel model scenarios. The distribution of $\lambda(m)$ along with the model created to approximate these distributions is shown in Fig. 1. Since $\lambda(m)$ versus m for the three channel environments considered are similar, we use a single model to represent $\lambda(m)$. This model is written as

$$\lambda(m) = \begin{cases} 1, & 1 \leq m \leq 2 \\ am^4 + bm^3 + cm^2 + dm + e, & 3 \leq m \leq 11 \end{cases} \quad (3)$$

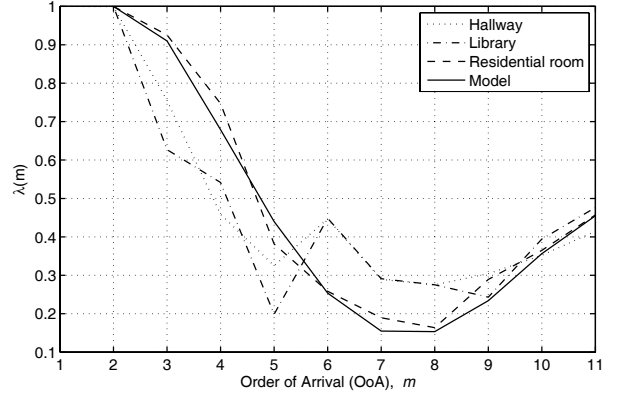


Fig. 1. The probability of each ray experiencing a single reflection before reaching the receiver for OoA index $m \leq 11$.

where $a = -0.001$, $b = 0.0289$, $c = -0.2488$, $d = 0.6251$, and $e = 0.5788$.

For the later-arrival paths ($m > 11$), the probability that they arrive at the receiver with an odd number of handedness-switched reflections is equal to $p_a = 0.5$. Therefore, for any m , the probability that a path will experience a significant cross-pol attenuation can be written as

$$p_a(m) = \begin{cases} 2p_s^2(\lambda(m)-1) - p_s(\lambda(m)-2), & 1 \leq m \leq 11 \\ 0.5, & m \geq 12. \end{cases} \quad (4)$$

We use the information obtained from (4) to modify the channel model (1) by creating a binary array of length 51 as

$$\mathbf{q} = [q_0 \ q_1 \ \cdots \ q_{50}] \quad (5)$$

where q_m takes on the values of A or 1 with probabilities $p_a(m)$ and $1 - p_a(m)$, respectively. The quantity A is the additional attenuation that the m -th ray experiences due to the cross-pol rejection of circular polarization. The special case of $A = 0$ corresponds to the theoretical case of infinite attenuation; a finite number corresponds to the more realistic cross-pol rejection (typically 15-20 dB). The value of q_0 , which corresponds to the direct path, is always equal to 1.

We can thus modify the channel model in (1) to incorporate the effect of circular polarization as

$$h(t) = a_{\text{Los}}q_0\delta(0) + \sum_{l=0}^{L-1} \sum_{k=0}^{K-1} a_{l,k}q_m\delta(t - T_l - \tau_{l,k}). \quad (6)$$

The value of m is related to k and l in a complex manner that depends T_l and $\tau_{l,k}$. Instead of dealing with this complex relation, we take a statistical approach for analysis and simulation. In this approach, we obtain the delay and fading coefficients of the paths using model (1), and then apply the modification vector given in (5).

Clearly, circular polarization will not work well in NLOS environments since the dominant reflected path must be exploited, rather than be suppressed with a non-zero probability. Also note that the special case with $q_m = 1, \forall m$, of the modified model (6) is simply the channel model for linear polarization.

III. SIMULATION

We simulate the bit-error rate (BER) performance of a system that employs pulse-shaped binary phase-shift keying

TABLE I
CHANNEL PARAMETERS USED IN SIMULATION

Parameter	Residential	Library	Hallway
Path loss exponent	1.53	3	2.29
Free space path loss intercept (dB)	75.1	50	69.7
Cluster arrival rate (1/ns)	1/4.76	0.25	1
Ray arrival rate (1/ns)	1/1.30	4	1
Cluster decay factor	4.19	12	1
Ray decay factor	1.07	7	7
Mean number of clusters	4	17	1
Handiness switching probability, p_s	0.45	0.24	0.26

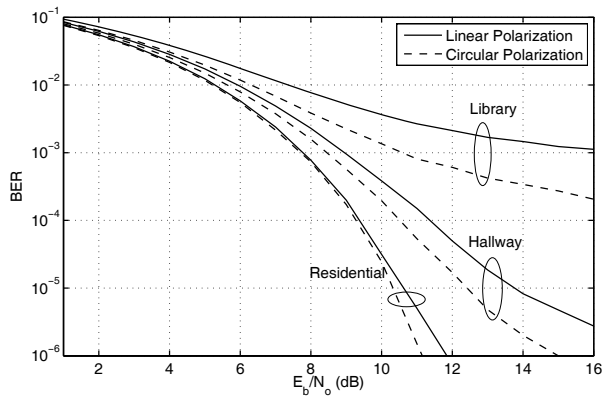


Fig. 2. BER performance of a BPSK system with linear and circular polarizations in various LOS environments. Square-root raised cosine filter is used with a roll-off factor of 0.3. 2000 blocks are simulated with a block length of 200 and 20 samples per symbol.

(BPSK) modulation and operates at a rate of 500 Mbps. The major parameters and values of the channel models are summarized in Table I; more related parameters can be found in [12]. We consider concrete as the reflective medium and the cross-pol rejection for receiver antennas is 20 dB for all propagation scenarios. The threshold of the incident angle is chosen to be $\theta_T = 50$ such that 10% or less power of the incident wave is reflected back with the same handiness. We obtain the probability distribution of θ_i from ray tracing, which considers 10^{10} different reflections for each application scenario. The values of p_s in Table I are obtained by $p_s = F_{\theta_i}(\theta_T)$, where $F_{\theta_i}(\cdot)$ was defined at the beginning of Section II-C.

Some common blocks of a wireless communication system such as channel coding and interleaving are not included so that we can clearly assess the impact of polarization on error rates of the raw data bits.

Fig. 2 shows the BER performance of the BPSK system in different LOS environments. For all scenarios, it is observed that circular polarization performs better than linear polarization in reducing the raw bit-error rates. The residential environment retains limited number of multipaths, with a delay spread of 0.1–0.2 ns; hence, the performance improvement due to circular polarization is insignificant. On the other hand, the library and hallway environments are severely affected by reflected paths and have a delay spread of a few ns. For these cases, the improvement in error performance due to the use of circular polarization in LOS environments is substantial, as clearly observed in Fig. 2.

IV. CONCLUSION

We have explored the error performance of 60 GHz wireless communications using different antenna polarizations. We first

extended the channel impulse response model developed for 60 GHz wireless communications with linear polarization to incorporate the effects of circular polarization. The statistics used in the extended model are obtained by ray-tracing simulation. Using the extended model, we then simulated the error performance of a coherent BPSK system with linear and circular polarizations in LOS environments. We found that in LOS environments, circular polarization reduces the multipath effect, and thus provides better performance than linear polarization approach, especially for systems operating at high data rates.

REFERENCES

- [1] H. Xu, V. Kukshya, and T. Rappaport, "Spatial and temporal characteristics of 60-GHz indoor channels," *IEEE J. Select. Areas Commun.*, vol. 20, no. 3, pp. 620–630, Apr. 2002.
- [2] A. Bourdoux, J. Nsenga, W. Van Thillo, F. Horlin, and L. Van der Perre, "Air interface and physical layer techniques for 60 GHz WPANs," in *Proc. Int. Symp. on Comm. and Veh. Tech.*, Nov. 2006, pp. 1–6.
- [3] H. Kim, K. Ahn, and H. Baik, "Phase noise suppression algorithm for OFDM-based 60 GHz WLANs," in *Proc. Int. ISWPC*, Jan. 2006, pp. 4.
- [4] T. Chen, H. Zhang, and I. Chlamtác, "High speed orthogonal waveform based indoor wireless transmission by a UWB and 60 GHz dual band system," in *Proc. ISWCS'06*, Sept. 2006, pp. 423–427.
- [5] H. El Ghannudi, L. Clavier, A. Bendjaballah, A. Boe, and P. Rolland, "Performance of IR-UWB at 60 GHz for ad hoc networks with directive antennas," in *Proc. IEEE ICUWB'06*, Sept. 2006, pp. 149–154.
- [6] S. Pinel, I. Kim, K. Yang, and J. Laskar, "60 GHz linearly and circularly polarized antenna arrays on liquid crystal polymer substrate," in *Proc. Euro. Microwave Conf.*, Sept. 2006, pp. 858–861.
- [7] S. Lei, S. Houjun, L. Deng, and C. Yong, "Study of the improved mm-wave omni-directional microstrip antenna," in *Proc. ISAPE'06*, Oct. 2006, pp. 1–4.
- [8] P. Smulders, "Broadband wireless LANs: a feasibility study," Ph.D. thesis, Eindhoven University of Technology, The Netherlands, ISBN 90-386-0100-X, 1995.
- [9] B. Langen, G. Lober, and W. Herzig, "Reflection and transmission behaviour of building materials at 60 GHz," in *Proc. IEEE PIMRC'94*, vol. 2, Sept. 1994, pp. 505–509.
- [10] K. Sato, *et al.* "Measurement of reflection and transmission characteristics of interior structures of office building in the 60-GHz band," *IEEE Trans. Antennas Propagat.*, vol. 45, pp. 1783–1791, Dec. 1997.
- [11] N. Moraitis and P. Constantinou, "Measurements and characterization of wideband indoor radio channel at 60 GHz," *IEEE Trans. Wireless Commun.*, vol. 5, no. 4, pp. 880–889, Apr. 2006.
- [12] S. Yong, "TG3c channel modeling sub-committee final report," IEEE 802.15-07-0584-00-003c, Jan. 2007 (<https://mentor.ieee.org/802.15/file/07/15-07-0584-01-003c-tg3c-channel-modeling-sub-committee-final-report.doc>).
- [13] J. Hubner, S. Zeisberg, K. Koora, J. Borowski, and A. Finger, "Simple channel model for 60 GHz indoor wireless LAN design based on complex wideband measurements," in *Proc. IEEE VTC'97*, vol. 2, May 1997, pp. 1004–1008.
- [14] T. Zwick, T. Beukema, and H. Nam, "Wideband channel sounder with measurements and model for the 60 GHz indoor radio channel," *IEEE Trans. Veh. Technol.*, vol. 54, no. 4, pp. 1266–1277, July 2005.
- [15] D. Matic, H. Harada, and R. Prasad, "Indoor and outdoor frequency measurements for MM-waves in the range of 60 GHz," in *Proc. IEEE VTC'98*, vol. 1, May 1998, pp. 567–57.
- [16] J. Kunisch, E. Zollinger, J. Pamp, and A. Winkelmann, "MEDIAN 60 GHz wideband indoor radio channel measurements and model," in *Proc. IEEE VTC'99*, vol. 4, Sept. 1999, pp. 2393–2397.
- [17] A. Sadri, A. Maltsev, and A. Davydov, "IMST time-angular characteristics analysis," IEEE 802.15-06-0141-00-003c, Mar. 2006 (<https://mentor.ieee.org/802.15/file/06/15-06-0141-01-003c-imst-time-angular-characteristics-analysis.ppt>).
- [18] F. Yildirim and H. Liu, "Directional MAC for 60 GHz using polarization diversity extension (DMAC-PDX)," in *Proc. IEEE Globecom07*, Nov. 2007.